CrystEngComm

Accepted Manuscript

This article can be cited before page numbers have been issued, to do this please use: B. Yan, P. Horton, A. E. Russell, C. J. Wedge, S. C. Weston and M. C. Grossel, *CrystEngComm*, 2019, DOI: 10.1039/C9CE00234K.

ROYAL SOCIETY OF CHEMISTRY

rsc.li/crystengcomm

View Article Online
DOI: 10.1039/C9CE00234K

Journal Name

COMMUNICATION

Crown ether alkali metal TCNQ complexes revisited – the impact of smaller cation complexes on their solid-state architecture and properties

Bingjia Yan,[a] Peter N. Horton,[a] Andrea E. Russell,[a] Christopher J. Wedge,[b] Simon C. Weston,[a] and Martin C. Grossel*[a]

Received 00th January 20xx,
Accepted 00th January 20xx

DOI: 10.1039/x0xx00000x

www.rsc.org/crystengcomm

The solid-state behaviour of four alkali metal TCNQ complexes: (15-crown-5)LiTCNQ (1), (15-crown-5)NaTCNQ (2), (15-crown-5)Li(TCNQ)$_2$·H$_2$O (3.H$_2$O) and (15-crown-5)Na(TCNQ)$_2$·H$_2$O (4.H$_2$O) has been explored by single crystal X-ray diffraction, Infrared (IR), Raman and Electron Paramagnetic Resonance (EPR) measurements. The presence of a small cation and ionophore leads to subtle changes in behaviour compared with their larger alkali metal analogues and in the hydrated salts water bridges form links between the crown-encapsulated cations and neighbouring TCNQ stacks.

Introduction

7,7',8,8'-Tetracyano-p-quinodimethane (TCNQ) is a good one electron acceptor which forms stable radical-anion salts ($M^+TCNQ^{\bullet-}$) with various metal, organometallic and organic cations.[1-7] In the solid-state, these salts often exhibit a range of electrical and magnetic properties,[8, 9] which are associated with the organisation of the paramagnetic $TCNQ^{\bullet-}$ moieties within the crystal architecture.[10-16] In particular, the $TCNQ^{\bullet-}$ units have a tendency to form face-to-face π-stacked dimers and infinite columns in the solid-state in which peripheral counter-cations are associated with the terminal cyano groups.[17-19] Furthermore, these anion stacks can incorporate neutral TCNQ units which can result in a significant change in their solid-state electronic properties.[20] The local geometry of the TCNQ dimer and its organisation within the crystal as a result of interaction with the counter-ion play an important role in determining the solid-state behaviour of such materials.[21] One approach for controlling this is through the use of ionophores such as crown ethers and cryptands. Nogami and co-workers[22, 23] reported the synthesis of a large number of ionophore-complexed metal TCNQ salts but no detailed structural characterisation was undertaken. We subsequently explored the solid-state behaviour of 18-crown-6 complexes of the K^+, Rb^+ and Tl^+ salts of $TCNQ^{\bullet-}$ and that of (15-crown-5)$_2$KTCNQ (**4**).[1, 17-19, 24, 25]

In the present study, we report the solid-state behaviour of the 15-crown-5 complexes of Li and Na TCNQ (**1**-**4**), and the effect of the presence of additional $TCNQ^0$ and water molecules on this.

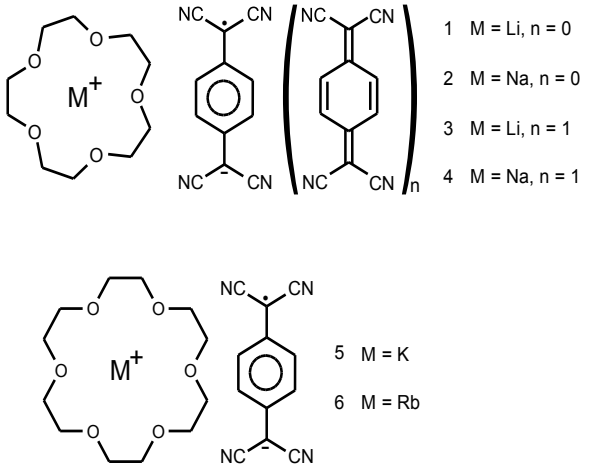

Figure 1. Structures of the TCNQ complexes discussed in this work

Experimental

General procedures

All experiments were performed under a nitrogen atmosphere unless stated otherwise. Acetonitrile was dried over calcium hydride and distilled before use. Diethyl ether was dried over sodium wire and was freshly decanted before use. All chemicals were commercially available and used as received, unless otherwise stated.

[a] School of Chemistry, University of Southampton, Highfield, Southampton, SO17 1BJ, UK. E-mail: M.C.Grossel@soton.ac.uk; Fax:+44 (0) 23 8059 3781; Tel: +44 (0) 23 8059 3153
[b] Department of Chemical Sciences, University of Huddersfield, Huddersfield, HD1 3DH, UK

† Electronic supplementary information (ESI) available: This contains the supplementary crystallographic and ESR data plus additional figures. CCDC reference numbers 1866252-1866256,. Full crystallographic data can be obtained free of charge from the Cambridge Crystallographic Data Centre via www.ccdc.cam.ac.uk/data_request/cif. For ESI and crystallographic data in CIF or other electronic format see DOI: XXXXXXXXXXXXXXXX.

Physical measurements

Melting points were determined on an electrochemical melting point apparatus and are uncorrected. Elemental analyses were performed by Medac Ltd, Chobham Business Centre, Chertsey Road, Chobham, Surrey, GU24 8JB. IR spectra (as KBr discs) were obtained using a Golden Gate sampling attachment on a Mattson Satellite 3000 FT-IR. Raman spectra were collected using a Renishaw In-Via system with a high powered near Infrared (HPNIR) 785 nm laser and microscope using a 50× objective. ESI mass spectra were obtained using a SolariX (Bruker Daltonics, Bremen, Germany) mass spectrometer equipped with a 4.7 T magnet and FT-ICR cell.

Single crystal X-ray diffraction

A suitable crystal was selected and measured following a standard method[26] on a *Rigaku AFC12* goniometer equipped with an enhanced sensitivity (HG) *Saturn724+* detector mounted at the window of a *FR-E+SuperBright* molybdenum (0.71075 Å) rotating anode generator with HF *Varimax* optics (70µm focus) (**1**, **3**, **4**) or (100µm focus) (**2**, **5**) at 100K. Cell determinations and data collections were carried out using *CrystalClear-SM Expert 3.1b27.*[27a] with data reduction, cell refinement and absorption correction carried out using *CrysAlisPro (v1.171.39.46)*[27b]. Structures were solved in Olex2[28] using S*HELXT*[29] and refined using *SHELXL*[30].

Electron paramagnetic resonance

All of the measurements were performed at X-band (~9.4 GHz) on a Bruker EMX EPR spectrometer using a cylindrical cavity (Bruker ER 4119HS or ER 4122 SHQE) and equipped with a programmable goniometer (ER 218PG1). Temperature control was achieved using nitrogen gas flow from a B-VT 2000 temperature controller with a quartz dewar insert (ER 169DIS). Microwave power was optimised to ensure signal response in the linear regime, typically requiring <1 mW. In some samples the presence of distinct species giving rise to signals of vastly different intensity and linewidth necessitated deliberate over-modulation of the narrower line.

General procedure for preparation of complexes (1) and (2)

A solution of the metal TCNQ salt (1 mol equiv) and 15-crown-5 (1 mol equiv) in anhydrous acetonitrile (50 ml) was boiled for 5 minutes, filtered whilst hot and then left to cool. The solvent was allowed to evaporate slowly at room temperature over a period of several days. During this time, a solid formed which was separated by filtration, washed with dry diethyl ether (50 ml), and then dried in vacuum to give the resulting small crystals.

Preparation of (15-crown-5)LiTCNQ (1)

Reaction of LiTCNQ (0.280g, 1.32mmol) with 15-crown-5 (0.291g, 1.32mmol) afforded small crystals of **1** as a purple solid (0.459g, 81%). MS (solution) (MeCN) (ESI^-) m/z: 204.1 ($TCNQ^{\bullet-}$). (ESI^+) m/z: 243.2 (Crown + Na^+). IR ν_{max}/cm^{-1} 2930, 2878 (saturated CH stretch), 2195, 2174, 2153 (CN stretch), 1579 ($C=C(CN)_2$ stretch), 1503 (C=C ring stretch), 1347 (CH bend), 1179 (C-CN and C-C ring stretch), 985 (C-C ring stretch), 829, 717 (CH out of plane bend). Raman ν_{max}/cm^{-1} 2216 (CN stretch), 1605 (C=C ring stretch), 1379 (C-CN stretch), 1208 (C=C-H bending). M.p. 202°C (dec.). Elemental analysis: Calculated: C: 61.25%, H: 5.61%, N: 12.98%. Found: C: 61.46%, H: 5.51%, N: 13.29%.

Preparation of (15-crown-5)NaTCNQ (2)

Reaction of NaTCNQ (0.450g, 2mmol) and 15-crown-5 (0.440g, 2mmol) gave small purple crystals of **2** (0.426g, 47.7%). MS (solution) (MeCN) (ESI^-) m/z: 204.1 ($TCNQ^{\bullet-}$). (ESI^+) m/z: 243.2 (Crown + Na^+). IR ν_{max}/cm^{-1} 2908, 2875 (saturated CH stretch), 2179, 2152 (CN stretch), 1576 ($C=C(CN)_2$ stretch), 1504 (C=C ring stretch), 1343 (CH bend), 1177 (C-CN and C-C ring stretch), 986 (C-C ring stretch), 820, 717 (CH out of plane bend). Raman ν_{max}/cm^{-1} 2207 (CN stretch), 1602 (C=C ring stretch), 1380 (C-CN stretch), 1205 (C=C-H bending). M.p. 160°C (lit.[22] 150°C). Elemental analysis: Calculated: C: 59.06%, H: 5.41%, N: 12.52%. Found: C: 58.76%, H: 5.02%, N: 12.32%.

Preparation of (15-crown-5)$Li(TCNQ)_2{\cdot}H_2O$ (3.H_2O)

Reaction of LiTCNQ (0.021g, 0.1mmol), $TCNQ^0$ (0.020g, 0.1mmol) and 15-crown-5 (0.044g, 0.2mmol) gave **3.H_2O** as blue crystalline plates (0.035g, 56%). MS (solution) (MeCN) (ESI^-) m/z: 204.1 ($TCNQ^{\bullet-}$). (ESI^+) m/z: 243.2 (Crown + Na^+). IR ν_{max}/cm^{-1} ~3500 (OH stretch), 2878 (saturated CH stretch), 2201, 2173 (CN stretch), 1560 ($C=C(CN)_2$ stretch), 1507 (C=C ring stretch), 1340 (CH bend), 1100 (C-CN and C-C ring stretch), 954 (C-C ring stretch), 836, 700 (CH out of plane bend). Raman ν_{max}/cm^{-1} 2216 (CN stretch), 1606 (C=C ring stretch), 1384 (C-CN stretch), 1206 (C=C-H bending). M.p. 270°C (dec.). Elemental analysis: Calculated: C: 62.48%, H: 4.63%, N: 17.14%. Found: C: 62.47%, H: 4.45%, N: 17.38%.

Preparation of (15-crown-5)$Na(TCNQ)_2{\cdot}H_2O$ (4.H_2O)

Reaction of NaTCNQ (0.028g, 0.1mmol), $TCNQ^0$ (0.020g, 0.1mmol) and 15-crown-5 (0.044g, 0.2mmol) afforded **4.H_2O** as blue crystalline plates (0.039g, 60%). MS (solution) (MeCN) (ESI^-) m/z: 204.1 ($TCNQ^{\bullet-}$). (ESI^+) m/z: 243.2 (Crown + Na^+). IR ν_{max}/cm^{-1} ~3500 (OH stretch), 2872 (saturated CH stretch), 2277, 2195, 2165 (CN stretch), 1560 ($C=C(CN)_2$ stretch), 1508 (C=C ring stretch), 1343 (CH bend), 1112 (C-CN and C-C ring stretch), 948 (C-C ring stretch), 836, 697 (CH out of plane bend). Raman ν_{max}/cm^{-1} 2206 (CN stretch), 1603 (C=C ring stretch), 1384 (C-CN stretch), 1206 (C=C-H bending). M.p. 252°C (dec.). Elemental analysis: Calculated: C: 60.98%, H: 4.52%, N: 16.73%. Found: C: 61.28%, H: 4.30%, N: 16.69%.

Preparation of (18-crown-6) K(TCNQ) (5)

This was prepared following the procedure reported previously to give **5** in 56% yield. M.p. 202°C (dec). (lit.[22] m.p. 203-205°C).

Results and discussion

Complexes of "simple" $TCNQ^{\bullet-}$ salts (1 and 2)

Crystallisation of Li or NaTCNQ from anhydrous acetonitrile in the presence of 15-crown-5 afforded dark purple single crystals suitable for X-ray structural study (at 100 K). In each case, a 1:1 complex of the metal $TCNQ^{\bullet-}$ salt with the crown ether was formed. The sodium salt showed solid-state behaviour similar to that seen previously for the 18-crown-6

complexes of K and RbTCNQ (**5** and **6** respectively),[19, 24] but that of the corresponding lithium salt showed significant differences. In order to facilitate analysis of the structural data, the structure of (18-crown-6)KTCNQ **5** was also re-determined at 100 K.

In the solid-state structure of (15-crown-5)NaTCNQ (**2**), the $TCNQ^{\bullet-}$ counterions form dimers in which diagonally opposite cyano groups on each $TCNQ^{\bullet-}$ unit are both co-ordinated to a sodium cation, this latter also being complexed within a crown ether cavity. The crown ether lies almost perpendicular to the $TCNQ^{\bullet-}$ molecular plane (see Fig 2). The top view of the TCNQ dimer (see Fig 2b) reveals that the $TCNQ^{\bullet-}$ dimer is significantly short-axis and slightly long-axis slipped (see Table 1 and Fig. 6 for key structural details).

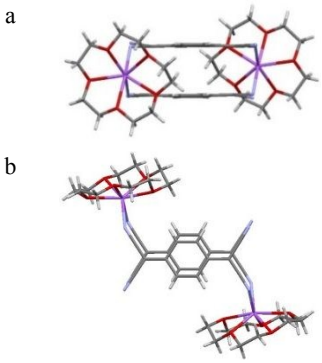

Figure 2. Side (a) and top (b) views of the dimer formed by (15-crown-5)NaTCNQ (**2**)

The dimers assemble into long-axis slipped extended columns (see Fig 3) similar to those previously observed in the 18-crown-6 complexes of K and RbTCNQ.[19, 24] However in the present structure, neighbouring TCNQ dimers within a column are closer to each other in comparison with their 18-crown-6 analogues reflecting the smaller volume of each dimer complex arising from the presence of the smaller crown ether. Perpendicular to these columns, the dimers form layers. The closest inter-dimer contact is 7.205(2) Å between the centroids of neighbouring $TCNQ^{\bullet-}$ dimer units within this structure [c.f. 8.1777(1) Å for the corresponding distance in (18-crown-6)KTCNQ **5** at 100 K].

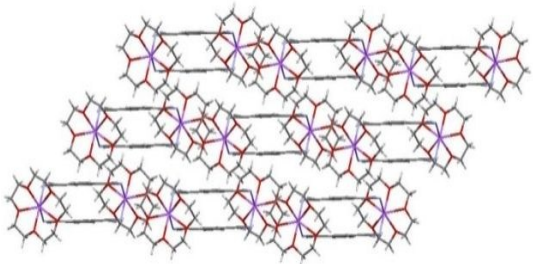

Figure 3. A side view of the extended columns of dimers in (15-crown-5)NaTCNQ (**2**)

For the (18-crown-6)K^+ complex **5**, neighbouring dimers within a layer are herringbone packed and the stacking axes of the associated $TCNQ^{\bullet-}$ columns are twisted relative to each other (by 60.86°).[18] However, in the sodium complex **2**, all of the neighbouring dimer planes and their stacking axes lie parallel with each other.

The solid-state behaviour of (15-crown-5)LiTCNQ **1** shows marked differences arising from the presence of the smaller lithium cation. Once again, a $TCNQ^{\bullet-}$ dimer is formed (see Fig 4) but in this case each $TCNQ^{\bullet-}$ is only directly coordinated to one lithium cation. Each $TCNQ^{\bullet-}$ unit has a slightly non-planar geometry with the non-coordinated $C(CN)_2$ termini twisted away from their dimer neighbours. The dimer components are significantly short-axis slipped (see Table 1 for key structural details).

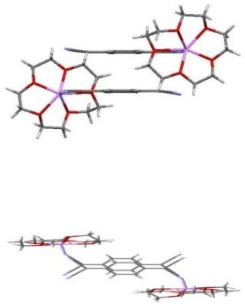

Figure 4 Side (a) and top (b) views of the dimer formed by (15-crown-5)LiTCNQ (**1**)

Another consequence of the reduced level of co-ordination to the $TCNQ^{\bullet-}$ dimer is that the location of the crown ether moieties is different; they now extend significantly above and below the plane of the $TCNQ^{\bullet-}$ dimer (see Fig 4a). The dimers assemble in sheets of parallel columns (see Fig 5a) but with the planes between neighbouring TCNQ dimers tilted at an angle of 48.63(7)° in a herringbone pattern (see Fig 5b).

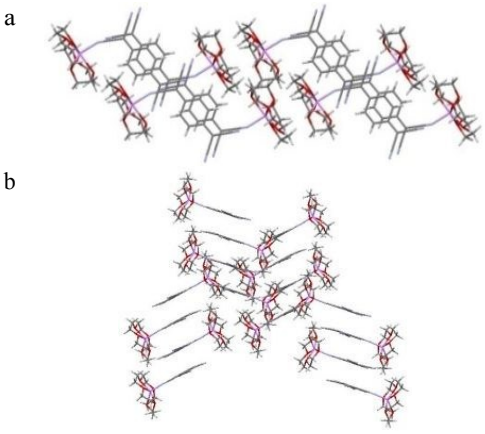

Figure 5. A sheet of dimer columns (a) and the herringbone packing arrangement of neighbouring sheets (b) in (15-crown-5)LiTCNQ (**1**)

Complex TCNQ salts (3 and 4)

Crystallisation of both Li^+ and Na^+ $TCNQ^{\bullet-}$ from anhydrous

View Article Online
DOI: 10.1039/C9CE00234K

acetonitrile in the presence of 15-crown-5 and one molar equivalent of $TCNQ^0$ afforded crystals of the complex salt (15-crown-5)M($TCNQ^{\bullet-}$)($TCNQ^0$)·H_2O (M = Li or Na) **3.H_2O** and **4.H_2O** respectively. Attempts to prepare crystalline samples of the anhydrous analogue of each of these materials failed.

Table 1. Key structural data for TCNQ dimers in the complexes discussed here with comparative literature data (see Fig.6 for definitions of long- and short-axis slip). Note that **3**,H_2O forms two different stacks (indicated as AA in green and BB in magenta in Figure 7).

Complex	π–π separation / Å	Long-axis slip / Å	Short-axis slip / Å	Reference
1 (at 100 K)	3.1501(13)	0.250(5)	0.964(5)	This work
2 (at 100 K)	3.2641(17)	0.176(8)	0.600(8)	This work
3.H_2O (AA) (at 100 K)	3.095(3)	2.141(11)	0.039(11)	This work
3.H_2O (BB) (at 100 K)	3.100(3)	1.946(10)	0.076(10)	This work
4.H_2O (at 100 K)	3.086(4)	2.058(16)	0.074(16)	This work
5 (at 100 K)	3.1559(7)	0.083(3)	0.532(3)	This work
5 (at Room temp)	3.2251(14)	0.080(6)	0.332(6)	Ref[17]
6 (at Room temp)	3.187(5)	0.081(19)	0.509(19)	Ref[24]

In the solid-state, the lithium complex (**3.H_2O**) forms a structure consisting of columns of TCNQ dimers in the channels between which lie (15-crown-5)Li(H_2O)$^+$ complexes. Each water molecule forms two significantly non-linear [C≡N···(H)O angle = 154.9(2)°] hydrogen-bonding contacts (2.00(5) and 2.05(5) Å) between TCNQ units in neighbouring columns (see Fig 7), only one cyano group from each TCNQ unit being involved. Similar behaviour has been observed in several hydrated lanthanide TCNQ salts.[31-34] These TCNQ columns consist of a 1:1 mixture of $TCNQ^0$ and $TCNQ^{\bullet-}$. The similarity of the bond lengths within the two TCNQ units and intra-./inter-dimer spacings makes it difficult to distinguish between the $TCNQ^{\bullet-}$ and $TCNQ^0$ components.

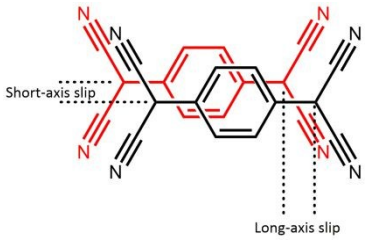

Figure 6. Definitions of short and long axis slip

The TCNQ dimers are significantly long-axis slipped with a π-π separation of 3.095(3)/3.100(3) Å (see Table 1), the terminal $C(CN)_2$ units being twisted relative to the benzenoid ring plane as a result of the hydrogen bonding to one of the cyano groups of each TCNQ component (see Fig 8).

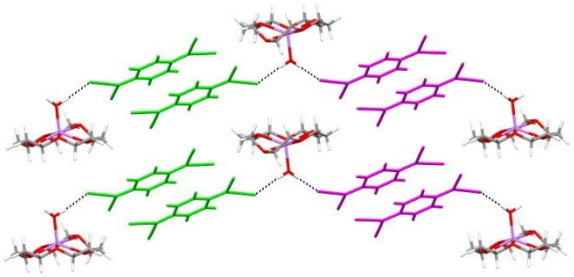

Figure 7. Water-bridged TCNQ columns formed by (15-crown-5)Li($TCNQ)_2$.H_2O (**3.H_2O**) (A stack in green and B stack in magenta)

In contrast with the other structures reported here, in the solid-state structure of the complex salt (15-crown-5) Na($TCNQ^{\bullet-}$)($TCNQ^0$)·H_2O (**4.H_2O**) the crown ether is disordered [as has been seen previously for [(15-crown-5)$_2K^+TCNQ^{\bullet-}$][1]. Once again, a water molecule is co-ordinated to the metal ion within the crown ether complex and forms a hydrogen-bonding contact with the nitrogen atoms of a TCNQ cyano group.

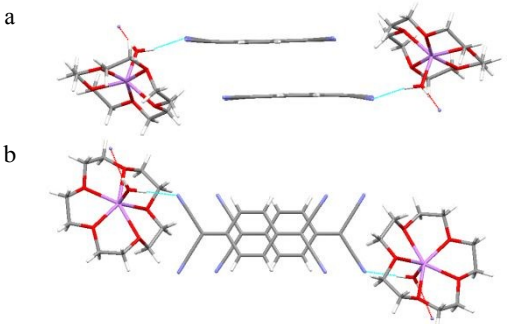

Figure 8. Side (a) and top (b) views of a TCNQ dimer unit showing in (15-crown-5)Li($TCNQ)_2$·H_2O (**3.H_2O**) showing hydrogen bonding contacts to adjacent Li^+-coordinated water molecules

The TCNQ units are dimerised within extended face-to-face π-stacked dimers which assemble into extended tetramers

View Article Online
DOI: 10.1039/C9CE00234K

forming parallel sheets throughout the structure separated by the crown ether complexes (see Fig 9).

Table 2. Infrared and Raman data for the TCNQ complexes reported in this work together with selected comparative literature data

Compound	Infrared data / cm^{-1}		Raman data / cm^{-1}			Ref.
	C≡N stretch	C=C stretch	C≡N stretch	C=C stretch	C-CN stretch	
$TCNQ^0$	2228, 2225	1545	2225	1600	1450	Ref,[38] Ref[39]
$TCNQ^0$	2224, 2220	1545	2230	1603	1454	This work
NaTCNQ	2197, 2184, 2160	1505	2204	1602	1384	This work
1	2195, 2174, 2153	1505	2216	1605	1379	This work
2	2179, 2152	1504	2207	1602	1380	This work
3.H_2O	2197, 2170	1507	2216	1606	1384	This work
4.H_2O	2196, 2167	1508	2206	1603	1383	This work
5	2201, 2187, 2177, 2158	1505	2197	1603	1388	This work
6	2202, 2187, 2177, 2158	1504	2197	1603	1388	Ref[41]

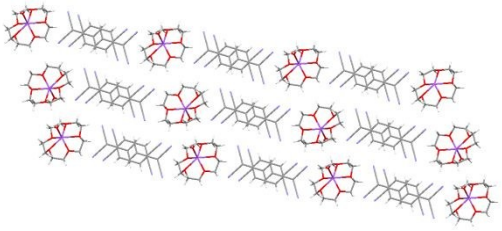

Figure 9. Top view of the sheets of face-to-face π-stacked columns of TCNQ dimers formed by (15-crown-5)$Na(TCNQ)_2{\cdot}H_2O$ (**4.H_2O**) showing the long-axis slipped nature of the TCNQ dimers. (*N.b.* For convenience the disordered nature of the crown ether is not shown)

Within each TCNQ dimer, the individual molecules are significantly long-axis slipped (see Fig 9) with a π-π separation of 3.086(4) Å (see Table 1). Once again, the water molecules apparently act as hydrogen-bonding bridges between neighbouring TCNQ columns thereby forming infinite hydrogen-bonded threads through the structure (see Fig 10).

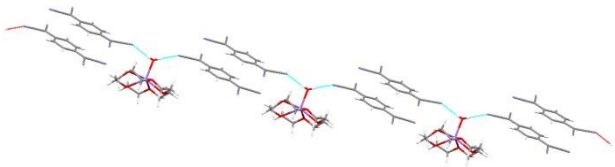

Figure 10. Water bridging hydrogen-bonded chains formed in (15-crown-5)$Na(TCNQ)_2{\cdot}H_2O$ (**4.H_2O**)

Vibrational spectra of Ionophore-encapsulated MTCNQ complexes 1-4

Infrared and Raman spectroscopy have previously been used to gain insight into the redox state of the TCNQ moiety.[35] Table 2 presents key data for complexes **1-6** together with some corresponding literature data for comparison. The spectra and number of bands reported here are consistent with previous literature reports.[36-39] We note the lack of sensitivity of the C≡N stretching vibrations to the changes in co-ordination environment observed in the crystal structures. This is easily accounted for by consideration of the angles of contact involved. To have a significant effect on ν(C≡N) a linear C≡N---M head-on contact is required. Variations in the number of cyano-bands observed is partially accounted for by the varying number of co-ordination environments seen in these structures.

Preliminary Electron Paramagnetic Resonance of Ionophore encapsulated MTCNQ salts

The behaviour of the complexes **1, 2, 3.H_2O** and **4.H_2O** has been studied by single crystal EPR Spectroscopy.

The EPR spectra of TCNQ salt **1** were recorded on multiple single crystals at temperatures up to 400 K. Two different spectral components were identified, one being a series of sharp lines observed at ambient temperature (see Fig S5), and of greater significance for the present discussion a strongly temperature dependent doublet as shown in Figure 11. The outer doublet is characteristic of a thermally populated triplet exciton, the two transitions of the $S = 1$ state being separated due to the fine structure splitting. Whilst these features are so broad that they are barely discernible at ambient temperature, the splitting decreases and the lines progressively narrow on heating until coalescing in a strong spectral singlet that dominates at high temperature, as seen previously for Frenkel-type triplet excitons.[10,40] A second behaviour characteristic of triplet exciton spectra is the change in line-width seen at certain orientations (see Fig S6). This has been attributed to interchain jumping of excitons between two crystallographically distinct chains at orientations in which they are magnetically equivalent in agreement[42] with our finding of two distinct dimer columns (see Fig 6).

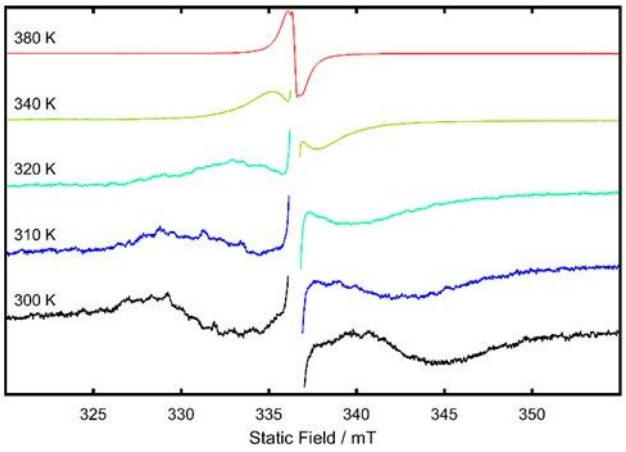

Figure 11. Temperature dependence of the EPR spectra of TCNQ salt **1** at a constant but arbitrary orientation. Spectra are individually scaled to highlight the triplet exciton signals, with the more intense central line omitted for clarity in all but the 380 K case. A high modulation depth of 300 μT is used to enable detection of the weak triplet exciton signals

The EPR behaviour of TCNQ salt **2** has also been explored over a temperature range 298–375 K. At ambient temperature, a central peak is observed whose field position is not orientation dependent, likely arising from a migrating exciton. As the temperature is increased to 315 K, a small doublet signal becomes apparent which was very weak at lower temperatures. The positions of these weak satellites signals change rapidly with crystal rotation exhibiting characteristics of a localised, thermally activated triplet state within the isolated $TCNQ^{\bullet-}$ dimer.[1, 17, 18, 25] Figure 12 shows the resulting roadmap as a function of angular displacement of TCNQ salt **2** at 315 K. This behaviour is similar to that previously reported for other crown ether-MTCNQ salt complexes, however only one doublet is observed for TCNQ salt **2** reflecting the presence of a single localised exciton due to the coplanar arrangement of the TCNQ dimers (see Fig 4). As illustrated for TCNQ salt **5** in Figure S7 for the previously reported 18-crown-6 K^+ and Rb^+ analogues, two independent doublets were observed due to the tilt angle between TCNQ dimer planes in neighbouring columns.[18] The orientation dependent splitting arises from the dipolar fine structure (zero-field splitting) of an excited triplet exciton state, and whilst a full determination of the spin-spin interaction tensor would require further data we can place a lower bound on the axial zero-field splitting parameter $|D_{Na}| \geq 426$ MHz making the value comparable to that for TCNQ salts **5** and **6**.

The electronic behaviour of TCNQ salts **3.H_2O** and **4.H_2O** has also been explored by variable-temperature EPR spectral experiments. In both cases, only a central feature can be observed with some weak anisotropy. As the temperature is increased signal intensity decreases, as expected for observation of a ground state doublet spin system obeying the Curie Law, in contrast to TCNQ salts **1** and **2** which showed the opposite behaviour with higher temperatures increasing the thermal population of triplet excited states and hence their signal intensity. There is no evidence for localised triplet excited states in either of TCNQ salts **3.H_2O** and **4.H_2O**, behaviour typical for other complex TCNQ salts in which there are extended mixed TCNQ stacks (i.e. containing both TCNQ and $TCNQ^{\bullet-}$).

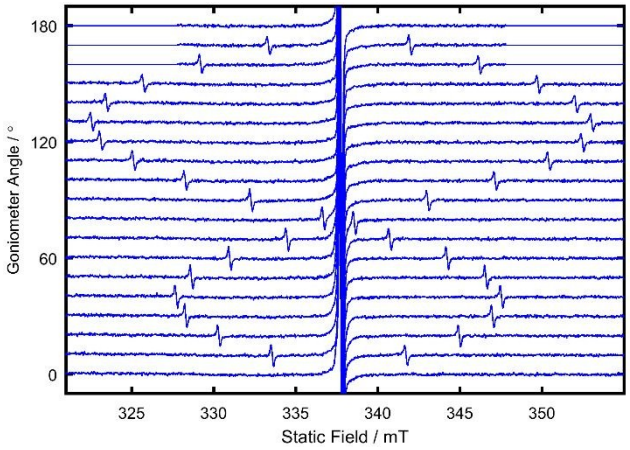

Figure 12. EPR Roadmap as a function of angular displacement of TCNQ salt **2** at 315K. Field modulation 200 μT

Conclusions

In the complexes involving simple (1:1) salts (**1** and **2**), the $TCNQ^{\bullet-}$ units form isolated $[TCNQ^{\bullet-}]_2^{2-}$ π-stacked dimers terminated by crown-encapsulated metal ions. Despite the reduced bulk of the Na^+(15-crown-5) complex, the solid-state behaviour of the sodium salt **2** mimics that of its 18-crown-6 potassium and rubidium analogues **5** and **6** respectively. In marked contrast, the behaviour of the lithium salt **1** is dominated by the limited co-ordination environment of the lithium cation with the result that each (15-crown-5)Li^+ unit is only associated with one cyano group of the TCNQ dimer. As Huang and co-workers[21] note, there are very few examples in the Cambridge Structural Database of assemblies of "isolated" TCNQ dimers such as those observed here for the simple $TCNQ^{\bullet-}$ salts **1** and **2** and the results obtained provide further insight into the behaviour of such dimers as the counter-cation co-ordination environment is modified. In marked contrast, the solid-state behaviour of the complex salts **3.H_2O** and **4.H_2O** is dominated by the presence of water-bridged hydrogen bonding to the TCNQ units there being no direct contact between these latter and the alkali-metal counter cation.

Notes and references

1. M. C. Grossel and S. C. Weston, *Chem. Mater.*, 1996, **8**, 977-980.
2. M. C. Grossel and S. C. Weston, *Contemp. Org. Synth.*, 1994, **1**, 367-386.
3. V. Kaminskii, R. Shibaeva and L. Atovmyan, *J. Struct. Chem.*, 1974, **14**, 1014-1019.
4. V. Kaminskii, R. P. Shibaeva and L. Atovmyan, *J. Struct. Chem.*, 1974, **14**, 646-650.
5. R. Shibaeva and L. Atovmyan, *J. Struct. Chem.*, 1972, **13**, 514-531.

6. R. Shibaeva, L. Atovmyan, V. Ponomarjev, O. Philipenko and L. Rozenberg, *Tetrahedron Lett.*, 1973, **14**, 185-188.
7. M. C. Grossel, P. B. Hitchcock, K. R. Seddon, T. Welton and S. C. Weston, *Chem. Mater.*, 1994, **6**, 1106-1108.
8. L. R. Melby, R. J. Harder, W. R. Hertler, W. Mahler, R. E. Benson and W. E. Mochel, *J. Am. Chem. Soc.*, 1962, **84**, 3374-3387.
9. J. G. Vegter, T. Hibma and J. Kommandeur, *Chem. Phys. Lett.*, 1969, **3**, 427-429.
10. D. B. Chesnut and W. D. Phillips, *J. Chem. Phys.*, 1961, **35**, 1002-1012.
11. D. B. Chesnut and P. Arthur, *J. Chem. Phys*, 1962, **36**, 2969-2975.
12. P. Nordio, Z. Soos and H. McConnell, *Annu. Rev. Phys. Chem.*, 1966, **17**, 237-260.
13. T. Hibma, P. Dupuis and J. Kommandeur, *Chem. Phys. Lett.*, 1972, **15**, 17-20.
14. T. Hibma and J. Kommandeur, *Phys. Rev. B*, 1975, **12**, 2608.
15. A. J. Silverstein and Z. G. Soos, *Chem. Phys. Lett.*, 1976, **39**, 525-530.
16. J. R. Morton, K. F. Preston, M. D. Ward and P. J. Fagan, *J. Chem. Phys.*, 1989, **90**, 2148-2153.
17. M. C. Grossel, F. A. Evans, J. A. Hriljac, K. Prout and S. C. Weston, *J. Chem. Soc., Chem. Commun.*, 1990, **0**, 1494-1495.
18. R. C. Hynes, J. R. Morton, K. F. Preston, A. J. Williams, F. Evans, M. C. Grossel, L. H. Sutcliffe and S. C. Weston, *J. Chem. Soc., Faraday Trans.*, 1991, **87**, 2229-2233.
19. M. C. Grossel and S. C. Weston, *J. Phys. Org. Chem.*, 1992, **5**, 533-539.
20. J. Lu, X. Qu, G. Peleckis, J. F. Boas, A. M. Bond and L. L. Martin, *J. Org. Chem.*, 2011, **76**, 10078-10082.
21. J. Huang, S. Kingsbury and M. Kertesz, *Phys. Chem. Chem. Phys.*, 2008, **10**, 2625-2635.
22. M. Morinaga, T. Nogami, Y. Kanda, T. Matsumoto, K. Matsuoka and H. Mikawa, *Bull. Chem. Soc. Jpn.*, 1980, **53**, 1221-1227.
23. T. Nogami, M. Morinaga, H. Mikawa, H. Nakano, M. Horioka, H. Horiuchi and M. Tokonami, *Bull. Chem. Soc. Jpn.*, 1990, **63**, 2414-2416.
24. M. C. Grossel, F. A. Evans, J. A. Hriljac, J. R. Morton, Y. Lepage, K. F. Preston, L. H. Sutcliffe and A. J. Williams, *J. Chem. Soc., Chem. Commun.*, 1990, **0**, 439-441.
25. M. C. Grossel and S. C. Weston, *J. Chem. Soc., Chem. Commun.*, 1992, **0**, 1510-1512.
26. S. J. Coles and P. A. Gale, *Chem. Sci.*, 2012, **3**, 683-689.
27. (a) CrystalClear, Rigaku Corporation, The Woodlands, Texas, U.S.A., (2008-2014); (b) CrysAlisPro Software System, Rigaku Oxford Diffraction, (2018).
28. O. V. Dolomanov, L. J. Bourhis, R. J. Gildea, J. A. Howard and H. Puschmann, *J. Appl. Crystallogr.*, 2009, **42**, 339-341.
29. G.M. Sheldrick, *Acta Crystallogr.,* 2015, **A71**, 3-8.
30. G. M. Sheldrick, *Acta Crystallogr., Sect. C: Struct. Chem.*, 2015, **71**, 3-8.
31. J.-W. Zhang, P.-F. Yan, G.-M. Li, B.-Q. Liu and P. Chen, *J. Organomet. Chem.*, 2010, **695**, 1493-1498.
32. H. Zhao, M. J. Bazile Jr, J. R. Galán-Mascarós and K. R. Dunbar, *Angew. Chem. Int. Ed.*, 2003, **42**, 1015-1018.
33. A. M. Madalan, H. W. Roesky, M. Andruh, M. Noltemeyer and N. Stanica, *Chem. Commun.*, 2002, 1638-1639.
34. J. Zhang, P. Yan, G. Li, G. Hou, M. Suda and Y. Einaga, *Dalton Trans.*, 2009, **0**, 10466-10473.
View Article Online
DOI: 10.1039/C9CE00234K
35. Z. Zhang, H. Zhao, M. M. Matsushita, K. Awaga and K. R. Dunbar, *J. Mater. Chem. C.*, 2014, **2**, 399-404.
36. (a) D. S. Acker and W. R. Hertler, *J. Am. Chem. Soc.*, 1962, **84**, 3370-3374. (b) J. S. Chappell, A. N. Bloch, W. A. Bryden, M. Maxfield, T. 0. Poehler, and D. 0. Cowan, *J. Am. Chem. Soc*, 1981, **103**, 2442-2443
37. A. Girlando, L. Morelli and C. Pecile, *Chem. Phys. Lett.*, 1973, **22**, 553-558.
38. R. Ramanathan, S. Walia, A. E. Kandjani, S. Balendran, M. Mohammadtaheri, S. K. Bhargava, K. Kalantar-Zadeh and V. Bansal, *Langmuir*, 2014, **31**, 1581-1587.
39. F. H. Herbstein and M. Kapon, *Crystallogr. Rev.*, 2008, **14**, 3-74.
40. A. Bencini and D. Gatteschi, *EPR of exchange coupled systems*, New York, Dover, 2012. (Original work published 1990, Berlin: Springer-Verlag)
41. S.C. Weston, PhD thesis, University of London, 1992.
42. Tj. Hibma and J. Kommandeur, *Phys. Rev. B*, 1975, **12**, 2608-2618.

Table of Contents Entry

View Article Online
DOI: 10.1039/C9CE00234K

Water molecules play a key structure-organising rôle in the crystallisation of 15-crown-5 complexes of Lithium and Sodium TCNQ in the presence of excess $TCNQ^0$.